Journal of Molecular Structure 1063 (2014) 219–225

Contents lists available at ScienceDirect

Journal of Molecular Structure

journal homepage: www.elsevier.com/locate/molstruc

3β-Acetoxy-6-nitrocholest-5-ene: Crystal structure, thermal, optical and dielectrical behavior

Shamsuzzaman [a,*], Ashraf Mashrai [a,1], Hena Khanam [a,1], Yahia Nasser Mabkhot [b], Wolfgang Frey [c]

[a] Steroid Research Laboratory, Department of Chemistry, Aligarh Muslim University, Aligarh 202002, UP, India
[b] Department of Chemistry, Faculty of Science, King Saud University, Riyadh 11451, Saudi Arabia
[c] Institut für Organische Chemie, Universität Stuttgart, Pfaffenwaldring 55, Stuttgart 70569, Germany

HIGHLIGHTS

- 3β-Acetoxy-6-nitrocholest-5-ene has been synthesized from 3β-acetoxycholest-5-ene.
- Structural assignment has been performed on the basis of FT-IR, FT-Raman, ^{1}H NMR, ^{13}C NMR, and X-ray crystallography.
- Thermal, optical, microstructural and dielectrical properties have also been explored.
- Thermal studies (TG–DTA–DSC) showed thermal stability and good crystalinity of the compound.

ARTICLE INFO

Article history:
Received 9 July 2013
Received in revised form 8 January 2014
Accepted 8 January 2014
Available online 30 January 2014

Keywords:
Steroid
X-ray
Thermal
Optical
Dielectrical

ABSTRACT

3β-Acetoxy-6-nitrocholest-5-ene (**2**) has been synthesized from 3β-acetoxycholest-5-ene (**1**). We provided an analysis of the compound by means of FT-IR, FT-Raman, NMR and X-ray crystallography. In addition microstructural, thermal, optical and dielectrical properties were also investigated. The compound **2** crystallizes in the monoclinic space group $P2_1$ with cell dimensions, a = 15.7729 (13) Å, b = 9.8933 (8) Å, c = 17.8070(14) Å, α = 90.00, β = 96.176(4), γ = 90.00. The powder X-ray diffraction (PXRD) of the compound was recorded to ascertain phase homogeneity. The SEM micrograph showed the presence of brick shaped, elongated nitrocholestane particles with 177.12 × 25.53 × 5.69 μm dimensions. Thermogravimetric analysis showed stability of the compound up to 200 °C. The dielectrical studies showed that with increase in frequency, the dielectric constant decreases and becomes almost constant at high frequencies.

1. Introduction

Steroids, a widespread class of natural organic compounds occurring in animals, plants and fungi, have shown great therapeutic value for a broad array of pathologies. They comprise a wide repertoire of structurally related natural compounds with important functions *in vivo*, such as physiological regulators, hormones, and provitamins. Steroids are representative of a rich structural molecular diversity and ability to interact with various biological targets and pathways. For the last seventy years the chemistry of steroids has provided one of the most interesting and thoroughly explored areas for organic chemists. The synthetic modification of naturally occurring steroids with the hope of improving pharmacological essentials has resulted in the preparation and discovery of a number of diverse pharmacologically active, potent, highly specific commercially important therapeutic agents [1–3]. Moreover steroids play an important biological role and have occupied a prominent position in medicinal chemistry field. Steroids have always attracted considerable interest because of their biological signaling molecules. Many representatives of this group are widely used in medicine as essentials of anti-inflammatory, diuretic, anabolic, contraceptive, antiandrogenic, progestational, anticancer and antimicrobial agents [4,5]. The steroidal drugs are widely used in traditional medicines, such as antibacterium, hormone kind medication, etc. Some steroid compounds are known to exert hormone receptor-independent antiproliferative activity via the inhibition of angiogenesis, tubulin polymerization and the upregulation of apoptotic pathways [6–8]. Cholesterol (Chol), a well known steroid, is ubiquitous in all living systems. Cholesterol is located in all membrane compartments at levels as high as 50-mole percent, which renders it the most prominent lipid in eukaryotic cells [9]. Cholesterol, which is synthesized de novo and obtained from the diet, largely affects the biophysical properties of cellular membranes and functions in a variety of synthetic pathways, including

* Corresponding author. Tel.: +91 9411003465.
E-mail address: shamsuzzaman9@gmail.com (Shamsuzzaman).
[1] These authors have contributed equally.

http://dx.doi.org/10.1016/j.molstruc.2014.01.031
0022-2860/

those of bile acids, hormones, and, through its precursor 7-dehydrocholesterol (7-DH-Chol), vitamin D synthesis [10]. Nitro compounds are very important and widely used chemicals [11] due to their versatile reactivities and simplicity to prepare. In particular, the nitro functionality can readily be introduced into a cholestane ring. The cholesteryl-nitro compound has been widely utilized as an intermediate for the preparation of 6-ketocholestane. In view of the aforementioned facts and in continuation of our programme on the synthesis of steroids [12], the present article embodies the spectroscopic and single crystal characterization of the 3β-acetoxy-6-nitrocholest-5-ene. In addition, dielectrical, thermal, morphological and optical behavior of the compound has also been explored.

2. Experimental section

2.1. General comments

All reagents and solvents were commercially available and used as received. Melting point was determined on a Kofler apparatus. The IR spectrum was recorded on KBr pellets with Interspec 2020 FT-IR Spectrometer spectro Lab and values are given in cm^{-1}. FT-Raman spectra were recorded on WITec alpha 300 scanning Near Field Optical Microscope (SNOM), Germany. ^1H and ^{13}C NMR spectra were run in $CDCl_3$ on a Bruker Avance II 400 NMR Spectrometer at 400 MHz and 100 MHz respectively. Chemical shifts (δ) are reported in ppm relative to the TMS (^1H NMR, 400 MHz) and to the solvent signal (^{13}C NMR spectra, 100 MHz). Elemental analyses of the compound were recorded on Perkin Elmer 2400 CHN Elemental Analyzer. X-ray diffraction (PXRD) pattern of powdered sample was recorded on MiniFlex™ II benchtop XRD system (Rigaku Corporation, Tokyo, Japan) operating at 40 kV and a current of 30 mA with Cu Kα radiation (λ = 1.54 Å). The diffracted intensities were recorded from 20° to 80° 2θ angles with scan rate of 2°/min and a step size of 0.02°. XRD measurements were performed at ambient temperature. The surface morphology of the compound was monitored using JEOL JSM-6510LV scanning electron microscope (SEM). Topographical images of the synthesized compound were taken using AFM, with a uniform thin film in acetonitrile on a 10 × 2.5 cm glass slide. To evaporate excess solvent, the slide was kept in vacuum at room temperature for 24 h. The sample was scanned using non-contact tapping mode and obtained 3D topological images. The thermal study of the compound was carried out using TGA/DTA-60H and DSC-60 instrument (SHIMADZU) at a heating rate of 20 °C min^{-1} from ambient temperature to 800 °C (for DSC 500 °C). UV–Vis spectrum was recorded on UV–Vis spectrophotometer (Perkin Elmer Life and Analytical Sciences, CT, USA) in the wavelength range of A200 to 700 nm. The fluorescence spectrum was collected at 37 °C with a 1 cm path length cell using a Hitachi spectrofluorometer (Model 2500) equipped with a PC and the emission slit were set at 5 nm. The emission spectrum was recorded in the range of 300–400 nm. The CD spectra of the crystal was collected a JASCOJ815 spectropolarimeter equipped with a Peltier-type temperature controller at 37 °C. Spectra were collected from 200 to 600 nm with 20 nm/min scan speed and a response time of 2 s. Respective blanks were subtracted. The Dielectric property was determined using impedance spectroscopy. The powder was pressed into pellets of 13 mm diameter and 0.84 mm thickness. Dielectric spectroscopy measurement was carried out in the frequency range 1 kHz to 1 MHz using LCR meter (Agilent 48). The pellets were coated on adjacent faces with silver paste, thereby forming parallel plate capacitor geometry. The value of dielectric constant (ε') is calculated using the formula, as follows: $\varepsilon' = c_p\, d/\varepsilon_o\, A$, Where, ε_o = permittivity of free space, d = thickness of pellet, A = cross sectional area of the flat surface of the pellet, c_p = capacitance of the specimen in Farad (F). Thin layer chromatography (TLC) plates were coated with silica gel G and exposed to iodine vapors to check the homogeneity as well as the progress of reaction. Sodium sulfate (anhydrous) was used as a drying agent.

2.2. Synthesis of 3β-acetoxy-6-nitrocholest-5-ene (**2**)

To a cooled mixture of cholesteryl acetate **1** (10 g) and conc. nitric acid (250 mL, d = 1.42) sodium nitrite (10 g) was gradually added with constant stirring over a period of about 45 min. After complete addition of sodium nitrite stirring was continued for additional 2 h. Cold water (300 mL) was added to reaction mixture, yellow solid material separated out. The whole mass was extracted with ether. The ethereal layer was washed with water, $NaHCO_3$ solution (5%) (until washings become pink), water and dried over anhydrous sodium sulfate. Removal of the solvents provided the nitro compound as oil which was crystallized from methanol to provide colorless crystals suitable for X-ray diffraction (Scheme 1) (yield: 6.5 g), m.p. 104 °C (reported m.p. 102–104 °C) [13]. Anal. Calc. for $C_{29}H_{47}NO_4$: C, 73.53; H, 10.00; N, 2.96 (%). Found: C, 73.50; H, 10.06; N, 2.90 (%); IR (KBr, cm^{-1}): 2944, 2869 (C—H, stretching), 1746 (C=O), 1519, 1301 (NO_2, stretching), 1464, 1365 (C—H, bending), 1237 (C—O); ^1H NMR ($CDCl_3$, 400 MHz): δ 4.72 (1H, m, C3α-H, $W_{1/2}$ = 16 Hz, axial), 2.01 (3H, s, $OCOCH_3$), 1.10 (3H, s, 10-CH_3) 0.67 (3H, s, 13-CH_3), 0.90 and 0.85 (other methyl protons); ^{13}C NMR ($CDCl_3$, 100 MHz): δ 170.1 (C=O), 150.2 (C-5), 148.1 (C-6), 72.1 (C—O), 56.2, 52.9, 49.3, 42.2, 41.1, 39.6, 39.2, 38.3, 38.1, 35.7, 34.7, 33.3, 32.7, 31.8, 30.1, 29.7, 28.7, 28.1, 27.9, 25.2, 23.2, 20.2, 19.2, 17.2, 12.1; MS (ESI): m/z 473.35 [$M^{+\cdot}$].

2.3. X-ray diffraction

Three dimensional intensity data for the compound **2** were collected at 100 K on Bruker KAPPA APEXII DUO diffractometer using Cu Kα radiation (λ = 1.54178 Å). The structure was solved by direct methods using SHELXS-97 software (SHELDRICK, 1990). Isotropic refinement of the structure by least-squares methods was carried out by using SHELXL-97 (SHELDRICK, 1997) followed by anisotropic refinement on F^2 of all the non-hydrogen atoms. Crystallographic data (excluding structure factors) for the structures reported in this article have been deposited with the Cambridge Crystallographic Data Centre (CCDC) as deposition No. CCDC 896096. All H-atom positions were calculated geometrically with U_{iso} (H) = 1.2–1.5 Å U_{eq} (parent atom). A riding model was used in their refinement (C—H = 0.98–1.00 Å).

3. Results and discussion

The experimental procedure followed in this manuscript [13] is almost similar to that reported by A.T. Rowland [11]. Here conc. nitric acid and sodium nitrite were taken without any other solvent while A.T. Rowland had used conc. nitric acid and potassium nitrite with ether as solvent.

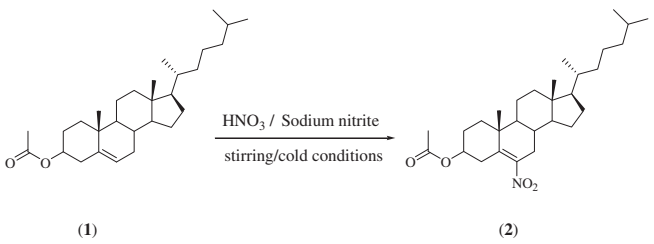

(**1**) (**2**)

Scheme 1. Synthesis of 3β-acetoxy-6-nitrocholest-5-ene.

3.1. FT-IR/Raman spectroscopy

The infrared spectral analysis provides useful information regarding the molecular structure of the compound. IR spectrum of compound **2** (Fig. S1) showed strong peaks at 1746 and 1234 cm^{-1} ascribed to C═O and C—O stretching vibrations respectively. The characteristic peaks observed at 1301and 1519 cm^{-1}, were assigned to ν (NO_2) stretching vibrations. The peaks at 1365 and 1464 cm^{-1}, corresponded to C—H bending mode of vibrations, whereby C—H stretching vibrations were detected at 2944–2869 cm^{-1}. The Raman spectrum of compound **2** in the 1250–3500 cm^{-1} spectral range is illustrated in Fig. S2. The spectrum demonstrated the position and relative intensity of the Raman bands. The spectrum displayed a strong band at 2750–3000 cm^{-1}, attributed to the stretching vibrations of the C—H units. A sharp medium peak around 1730 cm^{-1} was assigned to C═O stretching vibrations.

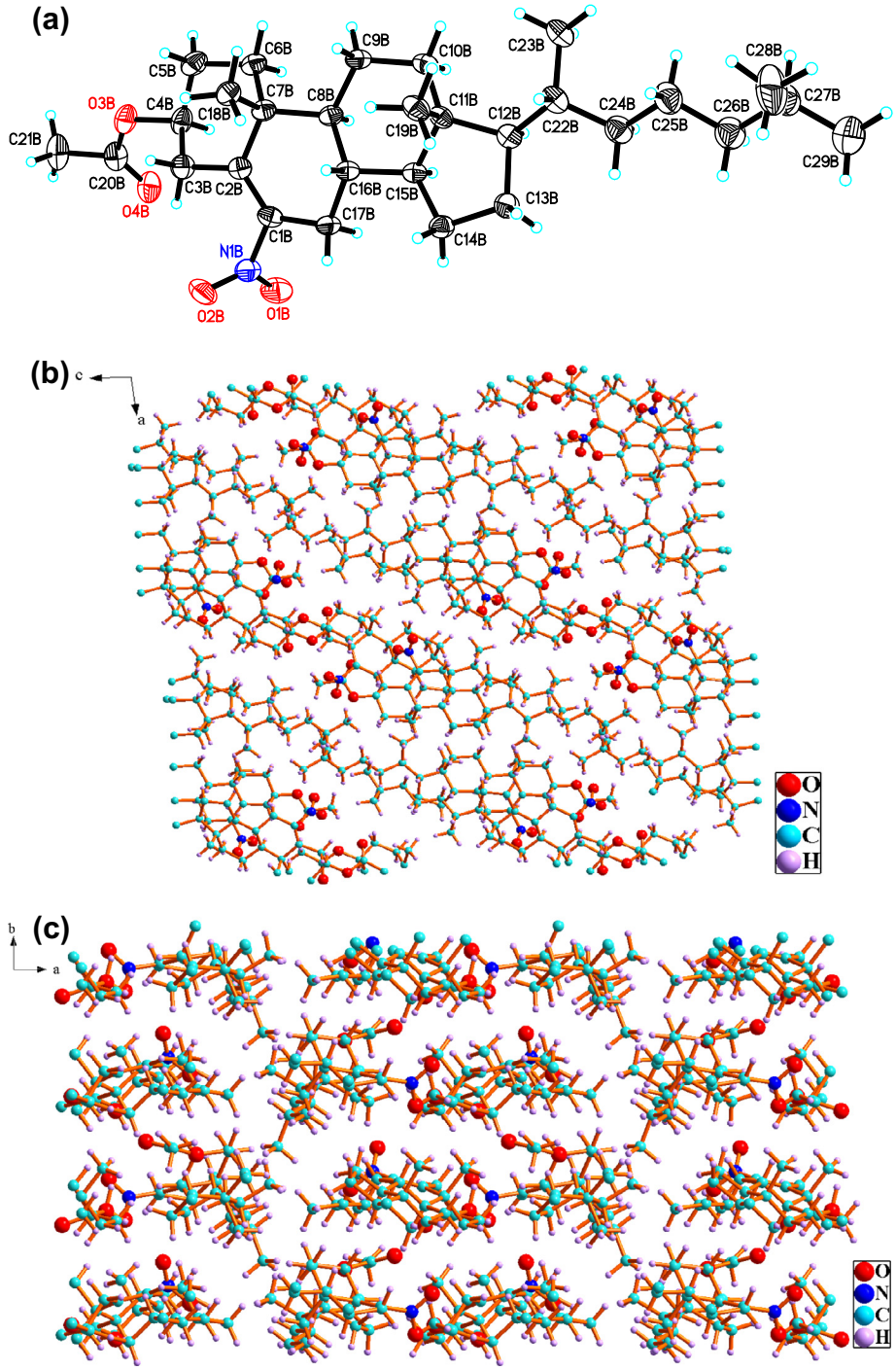

Fig. 1. 3β-Acetoxy-6-nitrocholest-5-ene (**2**): (a) a perspective view ellipsoid (50% Probability), (b) three-dimensional view along the *c* axis and (c) three-dimensional view along b axis.

3.2. NMR spectroscopy

NMR spectroscopy plays a vital role in the structural confirmation of the grown material. The NMR spectra (Figs. S3 and S4) of title compound showed a multiplet at δ 4.72 in ^{1}H NMR which was attributed to C3α-proton while three acetoxy protons appeared as a sharp singlet at δ 2.01. The half band width ($W_{1/2}$) value of C3-axial proton surely characterizes the junction of A/B ring as *trans* [4]. The characteristic peaks in ^{13}C NMR spectrum were obtained at δ 170.1 (C═O) and 72.1 (C—O). The chemical shift value of C-19 as δ 17.2 further conforms the nature of the ring junction [1].

3.3. Description of crystal structure

The title compound **2** crystallizes in the monoclinic system, space group $P2_1$ which can be explained by the presence of 8 *chiral* centers [14]. There are two molecules in the asymmetric unit, while unit cell contains 4 molecules (Figs. 1, S5 (a and b)) with the lattice constants of a = 15.7729 (13) Å, b = 9.8933 (8) Å, c = 17.8070(14) Å, and the detailed data are listed in Tables 1 and 2. The solvent molecule was not located in discrete locations in the crystal structure. Rings A and C exist in the chair conformation. Ring B adopts a half-chair conformation, and ring D is 11β envelope. The A/B ring junction is *quasi-trans*, while the B/C and C/D ring systems are *trans* fused about the C(8)—C(16) and C(11)—C(15) bonds, respectively. Ring bond lengths have normal values with an average of 1.528 (3) Å, while the cholestane side chain shows an average bond length of 1.521 (3) Å. The bond length C(1)—C(2) is 1.335 (3) Å, which indicates a double-bond character. The distance between acetoxy group and C4 is 1.456 (2) Å which is slightly longer than the average values reported [15]. The acetoxy group at position-4 is equatorial and antiperiplanar to the C5—C6 bond with a torsion angle 178.45° and the C1—NO_2 bond is 1.481(3) Å and the NO_2 group involved in two non covalent bonding (O2A···H10D, O1A···H15A Å) (Fig. S5(c)). The substitution at ring-A of the steroid nucleus causes significant changes in the bond distance and bond angle. The bond distances and bond angle in compound **2** are found to be C3—C4 = 1.518 (3) Å, C4—C5 = 1.509 (3) Å and C3—C4—C5 = 110.96 (18). The observed bond distances are shorter than the standard value of C(sp^3)—C(sp^3) bond [15]. The bond angles show some deviation from the average value of sp^3-type hybridization [16]. Side-chain is fully extended with a *gauche-trans* conformation of the terminal C28 and C29 methyl groups. There are eight *chiral* centres in the molecule, the absolute configuration of these sites were determined from the structure presented, these sites exhibit the following chiralities: C4 = S, C7 = R, C8 = S, C11 = R, C12 = R, C15 = S, C16 = S and C22 = R.

Table 1
Crystal data and structure refinement for crystal **2**.

Empirical formula	$C_{29}H_{47}NO_4$
Formula weight	473.68
Wavelength (λ)	1.54178 Å
Crystal system	Monoclinic
Space group	$P2_1$
Unit cell dimensions	
a (Å)	15.7729(13)
b (Å)	9.8933(8)
c (Å)	17.8070(14)
α (deg)	90.00
β (deg)	96.176(4)
γ (deg)	90.00
Volume (Å^3)	2762.6(4)
No. of molecules per unit cell (Z)	4
Calculated density, Mg m^{-3}	1.139
Absorption coefficient (μ, mm^{-1})	0.583
F(000)	1040
Crystal size	0.27 × 0.20 × 0.09 mm
θ range for data collection	2.50–66.59
Limiting indices	$-18 \leqslant h \leqslant 18$, $-11 \leqslant k \leqslant 9$, $-20 \leqslant l \leqslant 20$
Reflections collected	8175
Restraints/parameters	1/625
Goodness-of-fit on F^2	1.033
Final R indices [$I > 2\sigma(I)$]	R_1 = 0.0386, wR_2 = 0.0994
R indices (all data)	R_1 = 0.0439, wR_2 = 0.1015

$R_1 = \sum ||F_o| - |F_c|| / \sum |F_o|$ with $F_o^2 > 2\sigma(F_o^2)$. $wR_2 = [\sum w(|F_o^2| - |F_c^2|)^2 / \sum |F_o^2|^2]^{1/2}$.

Table 2
Selected bond lengths (Å) and angles (deg) for compound **2**.

Bond length	
O3B—C4B	1.456(2)
C4B—C5B	1.509(3)
C3B—C4B	1.518(3)
C1B—C2B	1.335(3)
N1B—C1B	1.481(3)
O1B—N1B	1.223(2)
N1B—O2B	1.225(3)
C1B—C17B	1.484(3)
Bond angle	
O1B N1B O2B	124.25(19)
O1B N1B C1B	116.76(18)
O2B N1B C1B	118.95(19)
C2B C1B N1B	118.97(18)
O3B C4B C5B	108.27(17)
C5B C4B C3B	110.96(18)
C1B C2B C3B	122.98(19)
N1B C1B C17B	112.10(16)

3.4. Powder XRD

The powder form of the grown crystal (**2**) was subjected to powder X-ray diffraction analysis. The appearances of sharp and strong peaks confirmed the good crystallinity of the grown crystals (Fig. 2). The lattice parameters of crystals were calculated using the powder XRD data and were found in good agreement with the values obtained from single crystals.

3.5. Microstructral studies (SEM/AFM)

3.5.1. Scanning electron microscopy

The surface morphology of the compound **2** was investigated by scanning electron microscopy (SEM). The SEM micrograph (Fig. S6) clearly showed the presence of brick shaped, elongated

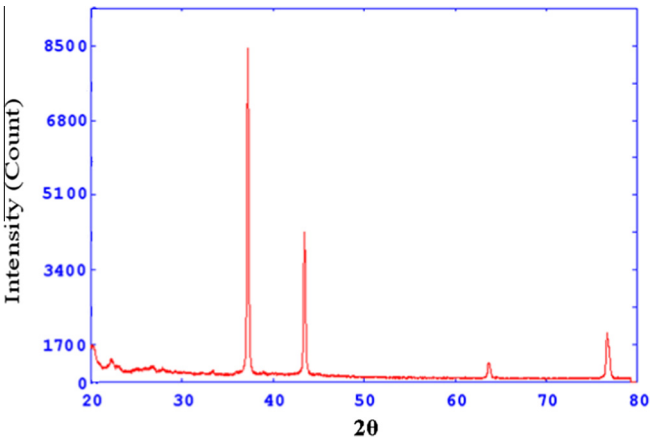

Fig. 2. Powder XRD of 3β-acetoxy-6-nitrocholest-5-ene (**2**).

nitrocholestane particles, extending over 177.12 μm in length, with few micro crystals on it.

3.5.2. Atomic force microscopy

The vertical and horizontal line analysis of images for the synthesized compound showed roughness parameters such as minimum and maximum surface value (Figs. S7 and S8). The mean value of the surface relative to the centre plane Mean roughness (Ra) value was found to be 12.23 nm. The other roughness parameters like mid-value (average of maximum and minimum), mean, peak to valley of the line (Rpv, difference between minimum and maximum), root-mean-squared roughness, ten point average roughness area (Rz, is the arithmetic average of the five highest and five lowest valleys peaks in the line calculated by ten point average), skewness (Rsk) and kurtosis (Rku) values of line are given in Table 3.

3.6. Thermal analysis (TG/DTA–DSC)

Thermogravimetric/differential thermal analysis/differential scanning calorimetry) (TG/DTA/DSC) measurements were performed under nitrogen atmosphere to examine the thermal stabilities of the crystalline sample and to define the conditions for the thermal treatment on it. Melting of the grown crystals had been estimated by differential thermal analysis (DSC). The thermograms observed from simultaneous TGA (Fig. 3) and DTA/DSC are illustrated in Figs. S9 and S10. The TG curve of compound **2** revealed that it is stable up to 200 °C (no weight loss) and does not undergo any phase transition. After 200 °C it started decomposition and 43.68% weight loss occurred at 260 °C and at 507 °C temperature 57.14% mass is lost. The disintegration process continued with the confiscation of almost all fragments as gaseous products, leading to the bulk decomposition of the compound before 700 °C since the initial mass of the sample was 5.308 mg and at a temperature of about 700 °C, all the mass was lost and nothing was left as residue. The absence of any weight loss or phase transition around or before its melting point, confirmed the nonexistence of any lattice entrapped solvent or moisture on the grown material as well as high stability of the steroidal nitro compound. The corresponding DTA curve showed three notable thermal events. The endothermic peak at 106 °C showed melting of the compound. The exothermic peaks at 306 °C and 600 °C depicted the crystallization of some of the phases of the decomposed material. From DSC (Differential scanning calorimetry) curve the melting point in the present investigation was found to be 102–104 °C.

3.7. Optical properties (Absorption spectra/fluorescence spectra/circular dichroism)

To determine the transmission range and to know the suitability of the crystals for optical applications, The UV–Vis absorption properties of compound **2** were recorded in dichloromethane solution with the concentration of 10^{-5} M. The absorption spectrum (Fig. 4) exhibited a strong, featureless absorption band around 265 nm, which can be assigned to an allowed $\pi \rightarrow \pi^*$ transition of the conjugated nitro-group with C=C double bond. Fluorescence

Table 3
AFM topographical mean surface parameters (nm) for compound **2**.

Line	Min.	Max.	Mid	Mean	Rpv	Rq	Ra	Rz	Rsk	Rku
Horizontal	−23.64	18.13	−4.14	0.00	42.70	12.50	10.59	24.50	0.30	2.01
Vertical	−14.52	14.21	−2.20	0.00	27.60	5.90	5.18	24.15	0.76	3.37

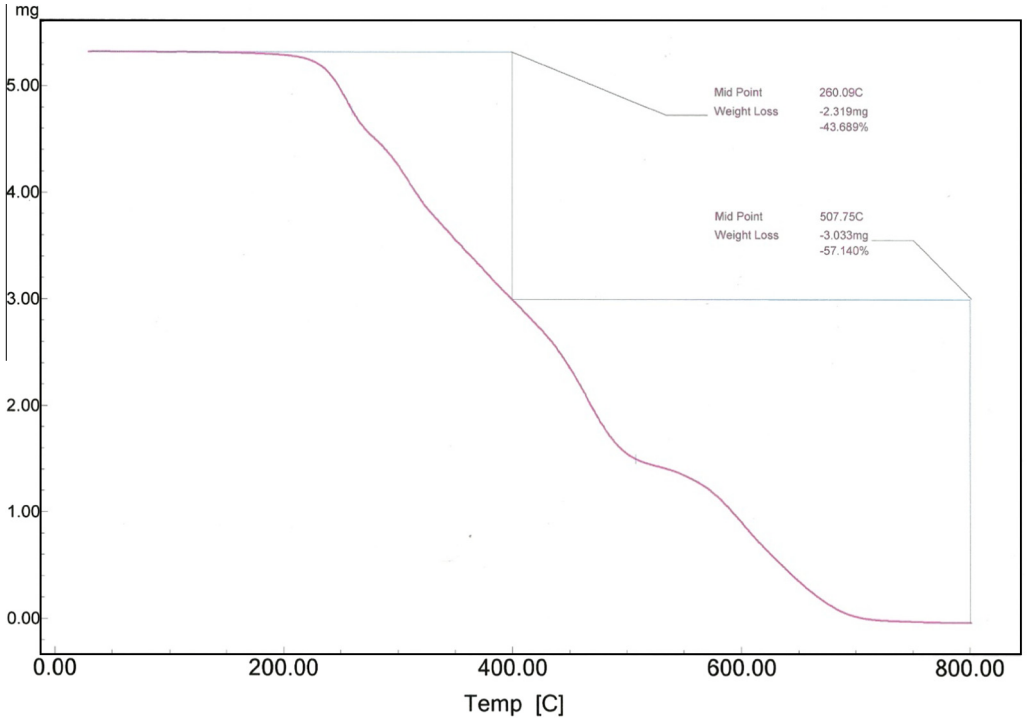

Fig. 3. TGA of 3β-acetoxy-6-nitrocholest-5-ene (**2**).

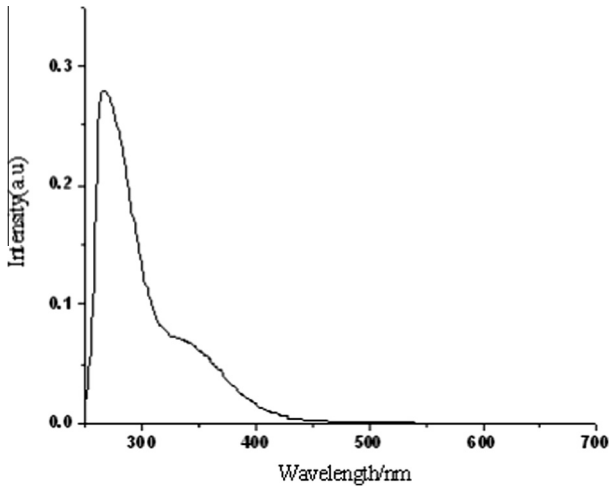

Fig. 4. UV–Vis spectrum of 3β-acetoxy-6-nitrocholest-5-ene (**2**).

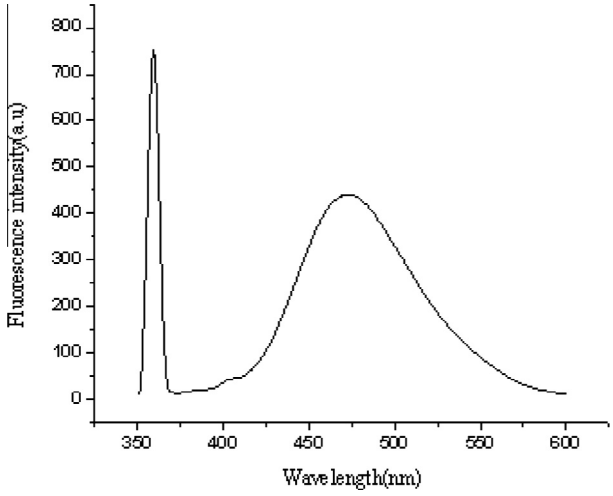

Fig. 5. Fluorescence spectrum of 3β-acetoxy-6-nitrocholest-5-ene (**2**).

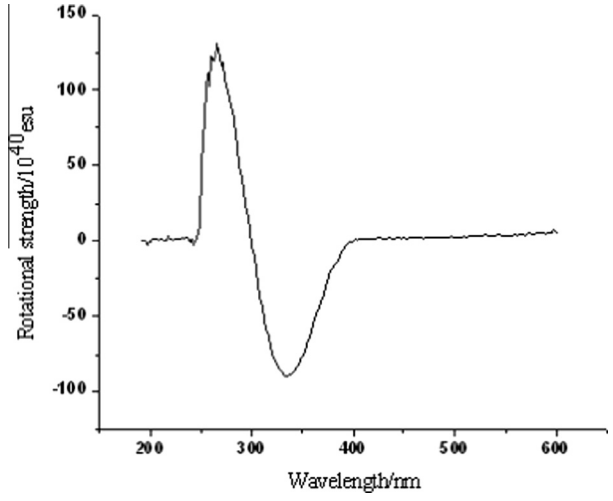

Fig. 6. CD of 3β-acetoxy-6-nitrocholest-5-ene (**2**).

image (Fig. 5) of the compound showed one sharp peak at 360 nm and another broad peak at 475 nm. The nitro-group is a chromophore which exhibits a Cotton effect while 3β-acetoxy-group of compound has no influence [17]. The conjugation of the nitro-group with a C=C double bond gives rise to intense ultraviolet absorption at about 266 nm, which has been classified as a charge-transfer band. The other band at 335 nm due to ($n \rightarrow \pi^*$) showed pronounced bathochromic shifts due to conjugation and no long wavelength band is detectable. The high circular dichroism is due to inherent dissymmetry of the chromophore (Fig. 6).

3.8. Dielectrical properties

The dielectric properties of the crystal was measured as a function of frequency at room temperature by equation $\varepsilon^* = \varepsilon' - i\varepsilon''$ where, ε' is real part of dielectric constant and describes the stored energy while ε'' is the imaginary part of the dielectric constant, which describes the dissipated energy. The dielectric constant is shown in *Fig.* S11. It is shown that with the increase in frequency, the dielectric constant decreases and becomes almost constant at high frequencies. This behavior can be explained using Maxwell–Wagner interfacial model. According to this model, a dielectric medium is considered to be composed of double layers, well conducting grains which are separated by poorly conducting or resistive grain boundaries. Under the application of external electric field, the charge carriers can easily migrate the grains but are accumulated at the grain boundaries. This process can produce large polarization and high dielectric constant. The higher value of dielectric constant can also be explained on the basis of interfacial/space charge polarization due to non-homogeneous dielectric structure.

4. Conclusion

3β-Acetoxy-6-nitrocholest-5-ene derived from corresponding cholest-5-ene has been characterized by spectral techniques. The lattice parameters have been determined by single-crystal X-ray diffraction analysis, which confirmed the identity of the synthesized material. The powder X-ray diffraction pattern (PXRD) of compound is equivalent to those simulated from single-crystal X-ray data. Thermal studies established that the compound undergoes no phase transition and is stable up to 200 °C. CD spectra showed intense ultraviolet absorption at about 266 nm, which has been classified as a charge-transfer band. The other band at 335 nm due to ($n \rightarrow \pi^*$) showed pronounced bathochromic shifts due to conjugation.

Acknowledgements

The authors would like to thank the Chairman, Department of Chemistry, Aligarh Muslim University, Aligarh for providing necessary research facilities. HK acknowledges UGC, New Delhi, India for providing BSR fellowship (R.No. Acad/D-742/MR). YNM thanks the Deanship of Scientific Research at King Saud University for the support (P.No. RGP-VPP-007). We are also thankful to Dr. Motohiro Nishio (The CHPI Institute, Japan) for his valuable discussion.

Appendix A. Supplementary material

Supplementary data associated with this article can be found, in the online version, at http://dx.doi.org/10.1016/j.molstruc.2014.01.031.

References

[1] Shamsuzzaman, H. Khanam, A. Mashrai, A. Sherwani, M. Owais, N. Siddiqui, Steroids 78 (2013) 1263–1272.
[2] B. Green, B.L. Jenseen, P.L. Lalan, Tetrahedron 34 (1978) 1633–1639.

[3] R.O. Clinton, A.J. Manso, J. Am. Chem. Soc. 83 (1961) 1478–1491.
[4] Shamsuzzaman, M.S. Khan, M. Alam, Z. Tabassum, A. Ahmad, A.U. Khan, Eur. J. Med. Chem. 45 (2010) 1094–1097.
[5] D. Kakati, R.K. Sarma, R. Saikia, N.C. Barua, J.C. Sarma, Steroids 78 (2013) 321–326.
[6] A.O. Mueck, H. Seeger, Steroids 75 (2010) 625–631.
[7] P. Verdier-Pinard, Z. Wang, A.K. Mohanakrishnan, M. Cushman, E.A. Hamel, Mol. Pharmacol. 57 (2000) 568–575.
[8] R. Minorics, T. Szekeres, G. Krupitza, B. Giessrigl, J. Wölfling, E. Frank, I. Zupkó, Steroids 76 (2011) 156–162.
[9] K.E. Bloch, CRC Crit. Rev. Biochem. 14 (1983) 47–92.
[10] L. Iuliano, Chem. Phys. Lipids 164 (2011) 457–468.
[11] A.T. Rowland, Steroids 26 (1975) 251–254.
[12] (a) Shamsuzzaman, H. Khanam, A. Mashrai, Y.N. Mabkhot, A. Husain, Acta Cryst. E68 (2012) o3037–o3038;
(b) Shamsuzzaman, A. Mashrai, H. Khanam, R.N. Aljawfi, Arab. J. Chem. (2013). http://dx.doi.org/10.1016/j.arabjc.2013.05.004;
(c) Shamsuzzaman, H. khanam, A. Mashrai, N. Siddiqui, Tetrahedron Lett. 54 (2013) 874–877.
[13] C.E. Anagnostopoulos, L.F. Fieser, J. Am. Chem. Soc. 76 (1954) 532–536.
[14] E. Pidcock, Chem. Commun. 27 (2005) 3457–3459.
[15] F.H. Allen, O. Kennard, D.G. Watson, L. Brammer, A.G. Orpen, R.J. Taylor, Chem. Soc. Perkin Trans. 2 (1987) S1–S19.
[16] Rajnikant, Dinesh, C. Bhavnaish, Acta Cryst. A62 (2006) 136–145.
[17] G. Snatzke, J. Chem. Soc. (1965) 5002–5015.